ACCOUNTS
of chemical research

# Endohedral Metallofullerenes Based on Spherical $I_h$-$C_{80}$ Cage: Molecular Structures and Paramagnetic Properties

TAISHAN WANG AND CHUNRU WANG*
*Beijing National Laboratory for Molecular Sciences, Key Laboratory of Molecular Nanostructure and Nanotechnology, Institute of Chemistry, Chinese Academy of Sciences, Beijing, 100190, People's Republic of China*

RECEIVED ON JULY 2, 2013

## CONSPECTUS

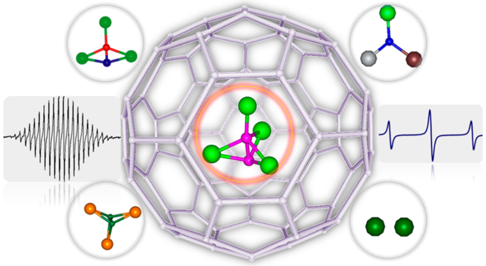

Fullerenes are carbon cages assembled from fused hexagons and pentagons that have closed networks and conjugated $\pi$ systems. The curve of the fullerene structure requires that the constituent carbon atoms take on a pyramidal shape and produces extra strain energy. However, the highly symmetrical geometry of the fullerene decreases the surface tension in these structures, so highly symmetrical fullerenes are usually very stable. For example, $C_{60}$ with icosahedral symmetry ($I_h$) is the most stable fullerene molecule. However, another highly symmetrical fullerene, $I_h$-$C_{80}$, is extremely unstable. The reason for this difference is the open-shell electronic structure of $I_h$-$C_{80}$, which has a 4-fold degenerate HOMO occupied by only two electrons. Predictably, once the degenerate HOMO of $I_h$-$C_{80}$ accepts six more electrons, it forms a closed-shell electronic structure similar to $I_h$-$C_{60}$ and with comparable stability. Because the hollow structure of fullerenes can encapsulate metal atoms and those internal metals can transfer electrons to the fullerene cage, the encapsulation of metal clusters may provide an ideal technique for the stabilization of the $I_h$-$C_{80}$ fullerenes.

In this Account, we focus on the molecular structures and paramagnetic properties of spherical $I_h$-$C_{80}$ endohedral fullerenes encaging a variety of metal moieties, such as metal atoms ($M_n$), metal nitride ($M_3N$), metal carbide ($M_nC_2$), metal carbonitride ($M_3CN$), and metal oxides ($M_4O_m$). We introduce several types of endohedral metallofullerenes such as $Sc_4C_2@I_h$-$C_{80}$, which exhibits a Russian-doll-like structure, and $Sc_3CN@I_h$-$C_{80}$, which encapsulates a planar metal carbonitride cluster. In addition, we emphasize the paramagnetic properties of $I_h$-$C_{80}$-based metallofullerenes, such as $Sc_3C_2@I_h$-$C_{80}$, $Y_2@C_{79}N$, and $M_3N@I_h$-$C_{80}$, to show how those spin-active species can present a controllable paramagnetism. This Account highlights an inspiring molecular world within the spherical $I_h$-$C_{80}$ cages of various metallofullerenes.

## 1. Introduction

Fullerenes are cage-shaped molecules composed of fused hexagons and pentagons with conjugated $\pi$ systems. In order to maintain the closure of each spherical network, each fullerene cage contains 12 pentagons to induce the curvature.[1] For example, $C_{60}$ has the highest $I_h$-symmetry with its 12 pentagons uniformly distributed on the fullerene cage, and this molecule is known to be the most stable fullerene until today.[2] However, it was found that not all highly symmetric fullerenes show high stability. In fact, the icosahedral fullerenes can be classified into two groups based on their electronic structures, in which the first one such as $C_{60}$ is stable with a fully occupied 5-fold degenerate HOMO and the second one, including $C_{20}$, $C_{80}$, etc., is less stable with a partially filled 4-fold degenerate HOMO.[3] For example, $C_{80}$ has seven isomers obeying the isolated-pentagon rule (IPR), that is, $D_{5d}$, $C_{2v-1}$, $D_2$, $C_{2v-2}$, $D_{5h}$, $D_3$, and $I_h$, in which the $I_h$-$C_{80}$ isomer was found to be the most unstable one.[3−5]

The unique empty cage structure of fullerenes enables them to accommodate one or several metal atoms or metal clusters, forming the endohedral metallofullerenes.[6−15] A pioneering study in metallofullerenes is the preparation of $La@C_{82}$,[16] in which three electrons are transferred from the endohedral lanthanum to the $C_{82}$ cage with an electronic structure being denoted as $[La]^{3+}@[C_{82}]^{3-}$. Undoubtedly,

10.1021/ar400156z

this type of charge transfer from the endohedral metal to outer cage opens up a road to stabilize the open-shell $I_h$-$C_{80}$. In 1995, the first stable $C_{80}$-based metallofullerene, $La_2@C_{80}$, was isolated and theoretically studied to own the $I_h$-symmetry.[17] Soon after, milligram scale of $La_2@I_h$-$C_{80}$ was obtained by improving the synthesis and isolation techniques,[18] and it was revealed that stable closed-shell $La_2@I_h$-$C_{80}$ is indeed formed via six electrons transferring from two lanthanum atoms to the $I_h$-$C_{80}$ cage characterized by $^{13}C$ NMR spectroscopy.

In 1999, the first metal nitride clusterfullerene, $Sc_3N@I_h$-$C_{80}$, was reported,[19] which brought the endohedral fullerenes to a new world of metallofullerenes. The following studies revealed that $Sc_3N@I_h$-$C_{80}$ is the third most abundant fullerene after hollow $C_{60}$ and $C_{70}$. In 2001, the metal carbide clusterfullerene $Sc_2C_2@C_{84}$ was reported, which further extends the metallofullerene family.[20] Since then more $I_h$-$C_{80}$-based metallofullerenes such as $Sc_3C_2@I_h$-$C_{80}$ with metal carbide,[21] $Sc_4O_2@I_h$-$C_{80}$ with metal oxide,[22] and $Sc_3CN@I_h$-$C_{80}$ with metal carbonitride[23] were revealed. Herein, we provide an overview of molecular structures and paramagnetic properties of these $I_h$-$C_{80}$-based endohedral metallofullerenes.

## 2. Icosahedral Symmetrical $C_{80}$ Cage

Figure 1a shows the structure of $I_h$-$C_{80}$, which has 12 pentagons and 30 hexagons. Hückel molecular orbital calculations suggest that the $I_h$-$C_{80}$ has a 4-fold degenerate HOMO ($a_g$, $b_{1g}$, $b_{2g}$, $b_{3g}$) occupied by two electrons and a 4-fold degenerate LUMO.[3,4,24] It is obvious that $I_h$-$C_{80}$ is very unstable due to its open-shell electronic structure; however, if the $I_h$-$C_{80}$ encages several metal atoms or a cluster to catch six extra electrons from the endohedral species, it would form a stable closed-shell electronic structure for $I_h$-$C_{80}$-based endohedral metallofullerene.

Moreover, it should be mentioned that the N-substituted $I_h$-$C_{80}$ cage, denoted as $C_{79}N$, has similar geometric structure except for an extra electron from the hetero N atom, so the $C_{79}N$ can be treated as analogue of $I_h$-$C_{80}$. In addition, due to an existing electron introduced by N atom, the $C_{79}N$ needs to accept only five electrons to reach stable closed-shell endohedral heterofullerenes.[25]

## 3. Various Endohedral Metallofullerenes Based on $I_h$-$C_{80}$

Because of the high symmetry and multifold degenerate frontier orbitals, $I_h$-$C_{80}$ fullerene cage is very favorable to construct metallofullerenes. On one hand, the highly symmetrical space of this fullerene cage enables it to encapsulate a large cluster without steric hindrance, for example, recently reported $Sc_4O_3@C_{80}$ has its internal species consisting of as many as seven atoms.[26] On the other hand, once the HOMO of $I_h$-$C_{80}$ is filled by six extra electrons from the encaged species, the resulting metallofullerenes would show very high stability. Therefore, the $I_h$-$C_{80}$ cage has a unique advantage in construction of various and stable metallofullerenes.

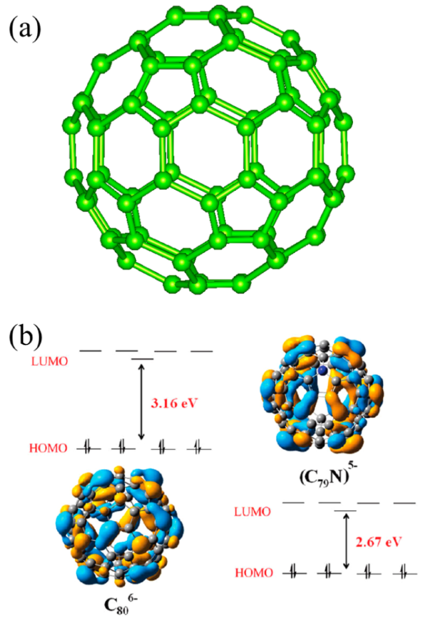

**FIGURE 1.** (a) Schematic structure of $I_h$-$C_{80}$. (b) DFT-calculated HOMO–LUMO levels of $(C_{80})^{6-}$ and $(C_{79}N)^{5-}$. Modified from ref 24.

The high symmetry of $I_h$-$C_{80}$ in endohedral metallofullerenes not only leads to their high stability but also induces a universal dynamic rotation of the internal species at room temperature. Reflected by the $^{13}C$ NMR spectroscopy, most $I_h$-$C_{80}$ in endohedral metallofullerenes reported so-far show a two-resonant-line profile with 3:1 ratio in intensity, corresponding to 60 corannulenic carbon sites and 20 triphenylenic carbon sites in $I_h$-$C_{80}$ cage. The results show that in these clusterfullerenes the endohedral clusters all can freely rotate and exhibit a uniform charge distribution within the $I_h$-$C_{80}$. In view of this, the structure of most $I_h$-$C_{80}$-based endohedral metallofullerenes can be basically determined by the $^{13}C$ NMR spectroscopy though other characterizations such as single crystal X-ray diffraction or IR/Raman spectroscopies are also required to unambiguously assign their structures.

**3.1. Metallofullerenes.** Traditional metallofullerenes based on $I_h$-$C_{80}$ encapsulating two metal atoms such as $Ce_2@I_h$-$C_{80}$ and $La_2@I_h$-$C_{80}$ have been widely studied.[8,18]

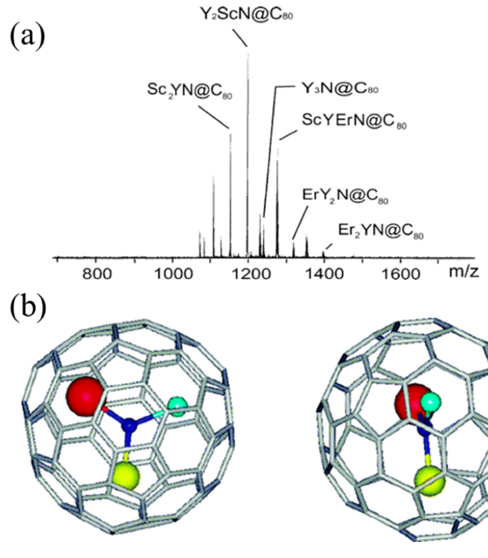

**FIGURE 2.** (a) MALDI-TOF mass spectrum of the TNT-clusterfullerene-containing fraction. (b) Schematic structures of $ScYErN@I_h$-$C_{80}$. Modified from ref 34.

Traces of $M_3C_{80}$ (M = Y, Dy, Sc) were also detected in the mass spectra of fullerene extracts, and the structure $Y_3C_{80}$ was predicted to have an $I_h$-$C_{80}$ cage by quantum calculations.[27] It was not until 2013 that the first trimetallofullerene $Sm_3@I_h$-$C_{80}$ was reported and characterized experimentally by single crystal XRD.[28] Computational studies demonstrated that the electronic features of $Sm_3@I_h$-$C_{80}$ are similar to those of theoretically studied $Y_3@I_h$-$C_{80}$, and both of them have a valence state of $[M_3]^{6+}@[I_h\text{-}C_{80}]^{6-}$. In these two species, the Sm and Y were calculated to adopt a formal +2 oxidation state. DFT calculations indicated that the HOMO is mainly localized on the cage and the LUMO is centered on the endohedral $Sm_3$ cluster, forming the so-called "interstitial" orbitals.[27,28]

**3.2. Metal Nitride Clusterfullerenes.** The family of endohedral metallofullerenes is largely extended by means of the so-called trimetallic nitride template (TNT) metallofullerenes, for example, $M_3N@I_h$-$C_{80}$ (M = Sc, Y, Lu, etc.) and $M_xL_{3-x}N@I_h$-$C_{80}$ (M, L = Sc, Y, Gd, Lu, etc.; $x = 0-3$). These structures and their properties have been intensively studied.[7-14,19,29-33] The $M_3N@I_h$-$C_{80}$ metallofullerenes also lead the preparations of many other TNT clusterfullerenes with non-$I_h$-$C_{80}$ cages.[10,13]

Because of the variable metal ion radius, these metal nitride clusterfullerenes show different structures and molecular properties. Especially for $M_3N@I_h$-$C_{80}$, the molecular electronic features can be gradually tuned by replacing one type of metal atom with another one to form the mixed-metal nitride clusterfullerenes. As shown in Figure 2, we designed and synthesized $ScYErN@C_{80}$, which has three different metal ions and one nitrogen encapsulated.[34] Moreover, the $ScYErN@C_{80}$ exhibits different electrochemical potentials from those in $Sc_3N@I_h$-$C_{80}$, $Y_3N@I_h$-$C_{80}$, and $Er_3N@I_h$-$C_{80}$. Considering that each metal element owns its unique property, this type of clusterfullerene may be designed as a multifunctional material to utilize in medical science.

**3.3. Metal Carbide Clusterfullerenes.** In 2005, a trimetal carbide clusterfullerene, $Sc_3C_2@I_h$-$C_{80}$, was structurally confirmed by $^{13}C$ NMR.[21] This interesting species has one unpaired electron that makes this molecule paramagnetic and NMR silent. Upon one-electron reduction, the anion of $Sc_3C_2@I_h$-$C_{80}$ becomes a closed-shell species whose $^{13}C$ NMR spectrum clearly exhibits the typical two signals in 3:1 ratio for $I_h$-$C_{80}$ cage. Density functional theory (DFT) calculations have shown that the $Sc_3C_2@C_{80}$ has a valence state of $[Sc^{3+}]_3[C_2]^{3-}@[I_h\text{-}C_{80}]^{6-}$.[35] Soon after, the $Sc_3C_2@I_h$-$C_{80}$ was investigated by synchrotron radiation X-ray powder diffraction, which revealed that the $Sc_3C_2$ cluster prefers a trigonal bipyramidal structure and exhibits a spherical charge distribution.[36] In 2007, another trimetal carbide clusterfullerene, $Sc_3CH@I_h$-$C_{80}$, was reported to encapsulate a hydrocarbon fragment in the cage.[37] The $Sc_3CH@I_h$-$C_{80}$ has a structure similar to that of $Sc_3N@I_h$-$C_{80}$ except for the bonded hydrogen, which makes the $Sc_3CH$ cluster slightly pyramidal. Furthermore, a valence state of $[Sc^{3+}]_3[CH]^{3-}@[I_h\text{-}C_{80}]^{6-}$ was disclosed by theoretical calculations.[37]

An important discovery in metal carbide clusterfullerenes should be ascribed to the report of $Sc_4C_2@I_h$-$C_{80}$ (Figure 3), which exhibits a Russian-doll-like nesting structure.[38] For this molecule, a $C_2$ unit is surrounded by a tetrahedron of four scandium atoms, and then this metal-carbide cluster is enveloped by an $I_h$-$C_{80}$ cage. $^{13}C$ NMR spectrum of $Sc_4C_2@I_h$-$C_{80}$ gives two signals with a ratio of 3:1, and this pattern reveals a highly symmetrical cage caused by free rotation of the endohedral $Sc_4C_2$ cluster. By quantum chemical calculations, $Sc_4C_2@I_h$-$C_{80}$ was revealed to possess a nested electronic structure of $[C_2]^{6-}@[Sc^{3+}]_4@[I_h\text{-}C_{80}]^{6-}$.[39] In $Sc_4C_2@I_h$-$C_{80}$, the HOMO is localized within the $Sc_4C_2$ cluster, whereas the LUMO is mainly delocalized on the carbon cage. These frontier orbitals and the peculiar $C_2^{6-}$ greatly influence the oxidation process of $Sc_4C_2@I_h$-$C_{80}$.[38]

**3.4. Metal Oxide Clusterfullerenes.** The first metal oxide clusterfullerene of $Sc_4O_2@I_h$-$C_{80}$ was synthesized and characterized in 2008, in which the $I_h$-$C_{80}$ cage encapsulates a distorted tetrahedron of $Sc_4$ with oxygen atoms positioned on the two triangular faces of $Sc_3$.[22] Soon afterward, the $Sc_4O_3@I_h$-$C_{80}$ encapsulating seven atoms was crystallographically

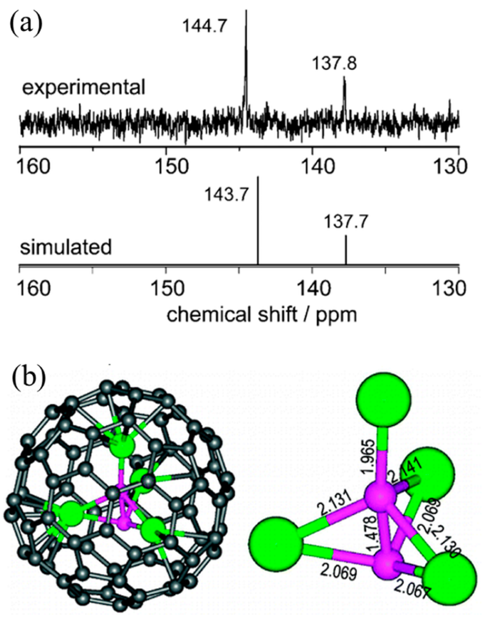

**FIGURE 3.** (a) Experimental and simulated $^{13}C$ NMR spectra of $Sc_4C_2@I_h$-$C_{80}$. (b) Optimized structure of $Sc_4C_2@I_h$-$C_{80}$. Green balls represent the Sc atoms and purple balls the carbon atoms of the inner $C_2$ moiety. Modified from ref 38.

determined to consist of a nearly tetrahedral $Sc_4$ with oxygen atoms bridging three triangular faces of $Sc_3$.[26] Theoretical computational studies indicated that the electronic structure of these two molecules can be formally described as $[Sc^{3+}]_2[Sc^{2+}]_2[O^{2-}]_2@[I_h\text{-}C_{80}]^{6-}$ and $[Sc^{3+}]_4[O^{2-}]_3@[I_h\text{-}C_{80}]^{6-}$.[40] In addition, in $Sc_4O_2@I_h$-$C_{80}$ the HOMO is largely confined to the $Sc_4O_2$ cluster; while in $Sc_4O_3@I_h$-$C_{80}$, the HOMO is largely delocalized over the fullerene cage.

### 3.5. Metal Carbonitride Clusterfullerenes.

In 2010, a trimetal carbonitride clusterfullerene, $Sc_3CN@I_h$-$C_{80}$, was synthesized in our group.[23] In its $^{13}C$ NMR spectrum, two signals at 144.9 and 137.7 ppm in a 3:1 intensity ratio were observed, which disclosed an $I_h$-$C_{80}$ cage and a rotational $Sc_3CN$ cluster. The structure of $Sc_3CN@I_h$-$C_{80}$ was unambiguously confirmed by single crystal X-ray diffraction, revealing the presence of the $I_h$-$C_{80}$ cage and a planar quinary $Sc_3CN$ cluster. The $^{45}Sc$ NMR spectrum for $Sc_3CN@I_h$-$C_{80}$ suggests a compact $Sc_3CN$ moiety with a free rotation inside the cage. Such peculiar dynamics of $Sc_3NC$ cluster enable the whole molecule to display a high polarity ($\mu = 2.42$ D).

Moreover, it should be noted that the endohedral C and N were not well identified by X-ray analysis; only theoretical calculations suggested that the isomer of $Sc_3CN@I_h$-$C_{80}$ with the C atom in the center of whole molecule has a lower energy than the N-centered isomer (Figure 4).[23,41] In 2013, the $Sc_3CN@I_h$-$C_{80}$ anion radical was successfully prepared, and its paramagnetic property was investigated.[42] It was revealed that when the center atom of $Sc_3CN$ was the C atom, the calculated hyperfine coupling constants (hfcc) fit better to the experimental results.

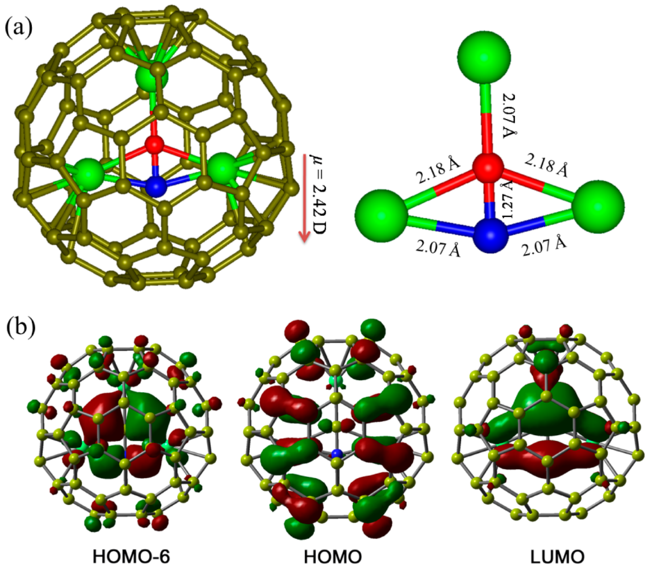

**FIGURE 4.** (a) DFT-optimized structure of $Sc_3CN@I_h$-$C_{80}$. Blue and red balls denote N and C atoms of the inner CN unit, respectively. (b) Selected molecular orbitals of $Sc_3CN@I_h$-$C_{80}$: HOMO − 6 (left), HOMO (middle), and LUMO (right).

The $Sc_3CN@I_h$-$C_{80}$ adopts a closed-shell electronic configuration with a valence state of $[Sc^{3+}]_3[CN]^{3-}@[I_h\text{-}C_{80}]^{6-}$.[41] Its LUMO is localized within the $[Sc_3CN]^{6+}$ cluster, whereas its HOMO is mainly contributed from carbon cage. Notably, its HOMO − 6 mainly consists of the in-plane $\pi^*$ orbital of $CN^{3-}$ and the $3d_\pi$ atomic orbitals of $Sc^{3+}$ cations, showing a covalent dative bond within $Sc_3CN$. Recently, similar metal carbonitride encapsulated metallofullerenes, that is, the $Sc_3CN@C_2(22010)$-$C_{78}$ with triscandium carbonitride,[43] and $YCN@C_{2v}$-$C_{82}$[44] with monoyttrium cyanide, were reported, suggesting the diversity of metallofullerenes with metal carbonitride clusters.

### 3.6. Dimetal Heterofullerenes.

A remarkable achievement in fullerene chemistry is the success of substituting one or more cage carbon atoms with heteroatoms such as $C_{59}N$.[45] However, this heterofullerene is highly reactive due to the exposed unpaired electron on the outer heteroatom. In 2008, the successful preparations of $M_2@C_{79}N$ (M = Y, Tb) were reported.[25] The crystallographic data for $Tb_2@C_{79}N$ clearly revealed an outer cage with nearly the same geometry as that of $I_h$-$C_{80}$. Moreover, theoretical calculations of $Y_2@C_{79}N$ revealed that the endohedral $Y_2$ unit offer five valence electrons to the cage, and the resulting $[C_{79}N]^{5-}$ is isoelectronic with $[I_h\text{-}C_{80}]^{6-}$. Unlike the $C_{59}N$ whose spin centers upon the outer N atom, the unpaired spin in $Y_2@C_{79}N$ locates at the inner $Y_2$

cluster and is protected by the heterofullerene cage. Besides, a recently reported $La_3N@C_{79}N$ and $Gd_2@C_{79}N$ further extended this family of endohedral heterofullerenes.[24,46]

## 4. Size Effect in Clusterfullerenes Based on $I_h$-$C_{80}$

As mentioned above, the $M_3N@I_h$-$C_{80}$ mode has superiority to gradually tune molecular properties by replacing metal atoms. For clusterfullerenes, the size of internal species varies largely depending on the ionic radii of metal, such as $Sc^{3+}$ (0.75 Å), $Lu^{3+}$ (0.85 Å), $Y^{3+}$ (0.90 Å), $Dy^{3+}$ (0.91 Å), or $Gd^{3+}$ (0.94 Å). It was revealed that the regioselectivity of exohedral cycloadditions for $I_h$-$C_{80}$-based clusterfullerenes is remarkably affected by the size of endohedral cluster. For example, the Prato reactions of $Sc_3N@C_{80}$ and $Y_3N@C_{80}$ lead to different fulleropyrrolidines with [5,6] and [6,6] sites revealed by experiments and calculations, respectively.[30−33,47]

In order to finely tune the electronic properties of clusterfullerenes, we designed and synthesized a series of mixed-metal nitride clusterfullerenes $Sc_{3-x}Y_xN@I_h$-$C_{80}$ ($x = 0-3$).[48] The four species have similar electronic structure, $(Sc_{3-x}Y_xN)^{6+}@(C_{80})^{6-}$, but the relatively larger ion radius of yttrium than that of scandium induces a gradually increasing size of endohedral clusters from $Sc_3N$, to $Sc_2YN$, to $ScY_2N$, and to $Y_3N$. It was found that the $Sc_3N@C_{80}$ fulleropyrrolidine in the Prato reaction favors [5,6] addition, and an obvious change in fullerene regioselectivity occurs at $ScY_2N@C_{80}$ fulleropyrrolidine where regioisomer with [6,6]-site appears, and the [6,6] addend finally becomes the major regioisomer in the case of $Y_3N@C_{80}$ fulleropyrrolidine. Similar regioselectivity for Prato reaction was found in $Sc_{3-x}Gd_xN@I_h$-$C_{80}$ ($x = 0-3$).[49] Moreover, experimental results disclosed an isomeric conversion when heating up the $ScGd_2N@C_{80}$ and $Gd_3N@C_{80}$ fulleropyrrolidines between [5,6] and [6,6] regioisomers.

To disclose the reason why the size of internal species of TNT metallofullerenes affect the regioselectivity of the $I_h$-$C_{80}$ cage, experiments and theoretical calculations were employed to study the internal size effect on the distortion of fullerene cage while encaging different clusters. A systematic $^{13}$C NMR studies on $Lu_xY_{3-x}N@I_h$-$C_{80}$ and $Lu_xSc_{3-x}N@I_h$-$C_{80}$ species all showed the typical two line $^{13}$C NMR profiles, but the chemical shift values of the TNT metallofullerenes exhibit upshift along with the expanding encaged clusters from $Y_3N$, $Y_2LuN$, $YLu_2N$, to $Lu_3N$ (Table 1).[50,51] Since the two NMR lines correspond to 60 corannulenic carbon sites and 20 triphenylenic carbon sites of $I_h$-$C_{80}$, it is reasonable to observe the corannulenic carbon sites bear more structural distortion than the rigid triphenylenic carbon sites, while increasing the size of TNT clusters. Moreover, the distortion of the fullerene cage was confirmed by the analysis of $\pi$-orbital axis vector (POAV) pyramidalization angles of the carbon atoms.[50,51]

**TABLE 1.** The $^{13}$C NMR Chemical Shifts of $Lu_xY_{3-x}N@I_h$-$C_{80}$

| clusterfullerenes | exptl $^{13}$C NMR chemical shifts (ppm) |
|---|---|
| $Y_3N@I_h$-$C_{80}$[51] | 138.04, 144.44 |
| $Y_2LuN@I_h$-$C_{80}$[51] | 137.95, 144.41 |
| $YLuN@I_h$-$C_{80}$[51] | 137.66, 144.22 |
| $Lu_3N@I_h$-$C_{80}$[51] | 137.39, 144.02 |

## 5. Paramagnetic Metallofullerenes Based on $I_h$-$C_{80}$

The $I_h$-$C_{80}$-based metallofullerenes always have their internal species free-rotating at room temperature as revealed by crystallography and $^{13}$C NMR spectroscopy.[19,21−23] In addition, crystallographic experiments showed that this kind of rotation can be influenced by low temperature and exohedral chemical modification.[21] Considering that the single crystal XRD analysis and $^{13}$C NMR measurement of clusterfullerenes are time-consuming, it is a challenge whether we can detect the dynamic rotation of internal species easily and manipulate it by other techniques. Recently, ESR was found to be a powerful tool in monitoring the movement of internal species.

More importantly, paramagnetic species based on endohedral metallofullerenes have attracted much attention because these ESR-active molecules are promising materials for molecule magnets and quantum information processing. The metallofullerenes based on $I_h$-$C_{80}$ have many paramagnetic molecules, such as $Sc_3C_2@I_h$-$C_{80}$, $M_3N@I_h$-$C_{80}$ with unpaired f-electrons embedded on metal ions, etc., and these molecules exhibit alluring and variable ESR properties. In the next part, we will illustrate the typical paramagnetic species, spin manipulation, and spin injection for the $I_h$-$C_{80}$-based metallofullerenes.

### 5.1. Paramagnetic Metallofullerenes Based on $I_h$-$C_{80}$.

$Sc_3C_2@I_h$-$C_{80}$ is an outstanding paramagnetic species based on $I_h$-$C_{80}$ cage, in which the unpaired electron is localized on the internal $C_2$ unit.[21,35] Its ESR spectrum shows 22 highly symmetrical lines caused by the interaction of unpaired spin with three equivalent Sc nuclei ($I = 7/2$). In paramagnetic $Y_2@C_{79}N$, the unpaired spin is mainly localized on the $Y_2$ dimer. Its ESR spectrum exhibits three symmetrical signals with 1:2:1 intensity ratio due to hyperfine couplings from two equivalent $^{89}$Y nuclei ($I = 1/2$) with large hfcc of 81.23 G.[25]

For lanthanide metal nitride clusterfullerenes, most of them have unpaired embedded spin on metal ions with partially filled f-shell. Different from the distinct ESR signals for Sc, Y, and La-containing clusterfullerenes, the ESR spectra of these f-spin-active clusterfullerenes should be measured under very low temperature. For example, the X-band ESR spectrum of $ErSc_2N@C_{80}$ was collected at 5 K, and the results revealed two different $Er^{3+}$ caused by varied orientations of the $ErSc_2N$ rotor.[52] For $Gd_3N@I_h$-$C_{80}$, the high-frequency ESR spectrum measured at 2 K showed broad 210 and 315 GHz ESR spectra caused by a single transition between the lowest Zeeman levels of static molecules.[53]

$TiM_2N@I_h$-$C_{80}$ (M = Sc, Y) clusterfullerenes are a new kind of typical paramagnetic molecules, which have an unpaired electron on $Ti^{3+}$ ion.[29,54] The $TiY_2N@I_h$-$C_{80}$ and $TiSc_2N@I_h$-$C_{80}$ both exhibit broad line width of ESR signals detected at room temperature. However, the line width of the ESR lines of $TiY_2N@I_h$-$C_{80}$ is much smaller than that of $TiSc_2N@I_h$-$C_{80}$, indicating two different paramagnetic structures caused by $Y_2$ and $Sc_2$ units.

**5.2. Spin Manipulation and Endohedral Dynamics.** The cycloadduct derivative of $Sc_3C_2@C_{80}$ with adamantylidene carbene ($Sc_3C_2@C_{80}$-Ad)[21] shows an ESR spectrum with hfcc of 7.39 G (two nuclei) and 1.99 G (one nucleus). Compared with three equivalent nuclei in pristine $Sc_3C_2@I_h$-$C_{80}$, the spin divergence in $Sc_3C_2@C_{80}$-Ad indicates a considerable influence of the exohedral modification on the molecular paramagnetism. Recently, a bisfulleroid derivative of $Sc_3C_2@C_{80}$ was reported to show different ESR parameters of 6.73 G (one nucleus) and 4.00 G (two nuclei) for the hfcc as well (Figure 5).[55] These results revealed an effective method of chemical modification to manipulate the electron spin features.

We made a detailed study of $Sc_3C_2@C_{80}$ fulleropyrrolidine.[56] The spin density of $Sc_3C_2@C_{80}$ fulleropyrrolidine is localized on the $Sc_3C_2$ inhomogeneously, which is very different from that of pristine $Sc_3C_2@C_{80}$ with homogeneous spin distributions on the $Sc_3C_2$ cluster. Apart from the spin divergence, a hindered rotation of the endohedral cluster was also concluded on the basis of the ESR study. The different hfcc of three nuclei in $Sc_3C_2@C_{80}$ fulleropyrrolidine show that the endohedral cluster cannot conquer the energy barrier to freely rotate again. By DFT calculations, oscillation modes around the equilibrium position were suggested.[56] The ESR studies of bis-adducts of $Sc_3C_2@C_{80}$ fulleropyrrolidines showed that the $Sc_3C_2$ cluster in bis-adducts display further restricted dynamics inside the cage.[57] These results disclosed a strong relationship between ESR properties and internal dynamics. Therefore, ESR spectroscopy will become a useful tool in monitoring the movement of endohedral species.

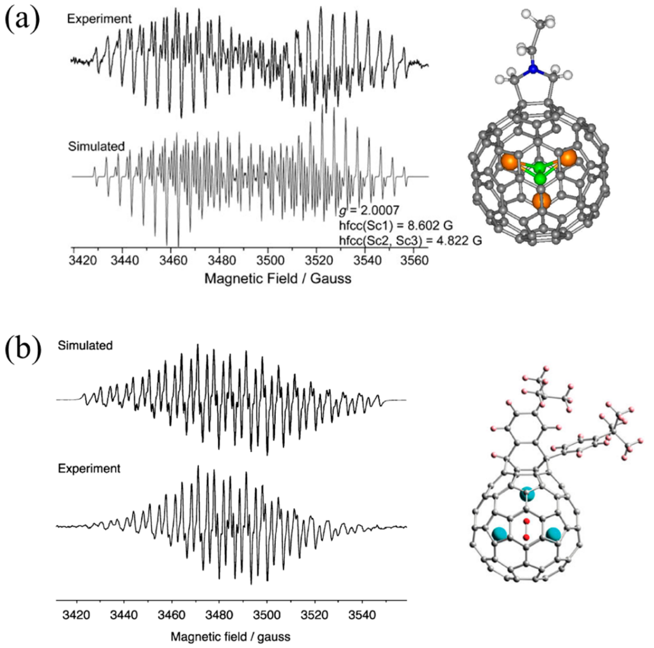

**FIGURE 5.** (a) ESR spectra and chemical structure of $Sc_3C_2@C_{80}$ fulleropyrrolidine. Panel a is modified from ref 56. (b) ESR spectra and chemical structure of $Sc_3C_2@C_{80}$ bisfulleroid. Panel b is modified from ref 55.

Besides chemical modification, the electron spin and dynamic rotation of internal species of $I_h$-$C_{80}$-based metallofullerenes can be manipulated by decreasing the temperature. We reported the highly impressionable electron spin in $Y_2@C_{79}N$ by modulating temperatures, indicating that the external stimulations may be employed to manipulate the spin-active $Y_2@C_{79}N$.[58] In the temperature-dependent ESR spectra of $Y_2@C_{79}N$, at room temperature three symmetrical signals were observed, while upon temperature decrease, the intensity of ESR signal in high magnetic field monotonously increases. This phenomenon can be ascribed to the paramagnetic anisotropy caused by a restricted rotation of the $Y_2$ moiety.

**5.3. Electron Spin Injection into Metallofullerenes Based on $I_h$-$C_{80}$.** Many clusterfullerenes have closed-shell structure and are ESR-silent, but electron spin can be introduced through chemical reduction or electrolysis. As a pioneer, the $Sc_3N@I_h$-$C_{80}$ anion radical was prepared by reduction of potassium and multilines with a large hfcc of 5.56 mT (55.6 G) were exhibited in its ESR specrum.[59] The injected electron spin of $Sc_3N@I_h$-$C_{80}^{-\bullet}$ was found to mainly locate on three scandium nuclei. Similar metal-based spin distributions were found in the cation and anion radicals of

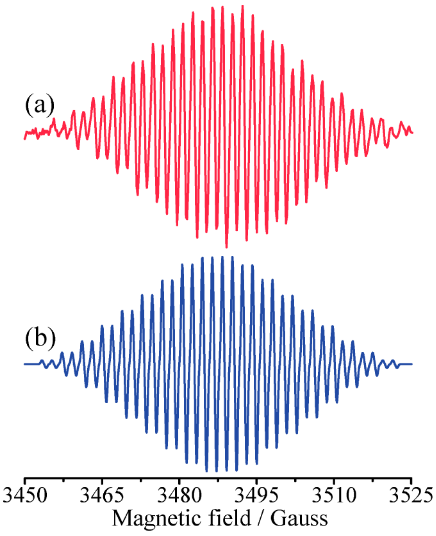

**FIGURE 6.** (a) Experimental and (b) simulated ESR spectra of $Sc_3NC@C_{80}$ anion radical. Reproduced from ref 42.

$Sc_4O_2@I_h$-$C_{80}$ generated electrochemically.[60] For the anion radical, two pairs of equivalent Sc atoms with hfcc of 2.6 and 27.4 G were concluded, and for cation radical, larger hfcc of 19.0 and 150.4 G was observed, indicating a significant effect of valence state on the ESR properties.

Recently, we prepared the anion radical of $Sc_3CN@I_h$-$C_{80}$ by reduction of potassium.[42] Its ESR results revealed hfcc of 3.890 G for two equivalent Sc nuclei and 1.946 G for the third Sc nucleus (Figure 6). Theoretical calculations disclosed that the unpaired spin is localized on the CN core moiety. Moreover, the C-centered $Sc_3CN@I_h$-$C_{80}$ structure was determined by theoretical calculations on hfcc compared with the experimental data for $Sc_3CN@I_h$-$C_{80}$ anion radical. These results reveal that the hyperfine couplings of ESR spectrum are very sensitive to the structure of clusterfullerene.

## 6. Conclusions

In this Account, we summarized some important endohedral metallofullerenes based on spherical $I_h$-$C_{80}$. The $I_h$-$C_{80}$ cage has been observed to have excellent ability to encage various kinds of metal atoms or metal-containing clusters and leads to many new structures of endohedral metallofullerenes. For example, the $Sc_4C_2@I_h$-$C_{80}$ exhibits an interesting Russian-doll-like structure, and the $Sc_4O_3@C_{80}$ demonstrates a complexity for endohedral moieties. The $I_h$-$C_{80}$-based metallofullerenes often lead the families of clusterfullerenes, such as $Sc_3N@I_h$-$C_{80}$ and $Sc_3CN@I_h$-$C_{80}$ for metal nitride and metal carbonitride clusterfullerenes, respectively. Furthermore, the $I_h$-$C_{80}$-based metallofullerenes always have their internal species free-rotating, and this characteristic gives them high symmetry and special stability. For $M_3N@I_h$-$C_{80}$, the size effects of endohedral clusters on molecular properties reveal significant interactions between the internal clusters and outer $I_h$-$C_{80}$ cage. For the paramagnetic $I_h$-$C_{80}$-based metallofullerenes, they have diverse and controllable ESR properties and are promising materials for molecule magnets and quantum information processing. From structures to properties, the metallofullerenes based on spherical $I_h$-$C_{80}$ cage display an inspiring molecular world, which will undoubtedly attract more attention in the future.

---

*We thank the National Basic Research Program (Grant 2012CB932900), National Natural Science Foundation of China (Grants 21121063, 21203205), NSAF (Grant 11179006), and China Postdoctoral Science Foundation (Grant 201104153).*

## BIOGRAPHICAL INFORMATION

**Taishan Wang** is a postdoctoral fellow in the Institute of Chemistry, Chinese Academy of Sciences. He received his B.S. at Shaanxi Normal University in 2005. Then he studied in Prof. Chunru Wang's group and got his Ph.D. in Physical Chemistry from Chinese Academy of Sciences in 2010. His research interests include the structures and paramagnetic properties of metallofullerenes and photoelectric functional fullerene materials.

**Chunru Wang** is a professor in the Institute of Chemistry at the Chinese Academy of Sciences. He received his B.S. at Inner Mongolian University and his Ph.D. in Physical Chemistry in 1992 from the Chinese Academy of Sciences. His research interests include the synthesis, isolation, and characterizations of endohedral fullerenes and the industrial applications of fullerenes and metallofullerenes. Recently, his group has developed a technique to produce gram-scale endohedral metallofullerenes for medical applications.

## FOOTNOTES

*Corresponding author. E-mail: crwang@iccas.ac.cn.
The authors declare no competing financial interest.

## REFERENCES

1 Fowler, P. W., Manolopoulos, D. E. *An Atlas of Fullerenes*; Clarendon Press: Oxford, U.K., 1995.
2 Hirsch, A., Brettreich, M. *Fullerenes: Chemistry and Reactions*; Wiley-VCH Verlag GmbH & Co. KGaA: Weinheim, Germany, 2005.
3 Khamatgalimov, A. R.; Kovalenko, V. I. Electronic structure and stability of $C_{80}$ fullerene IPR isomers. *Fullerenes, Nanotubes, Carbon Nanostruct.* **2011**, *19*, 599–604.
4 Furche, F.; Ahlrichs, R. Fullerene $C_{80}$: Are there still more isomers? *J. Chem. Phys.* **2001**, *114*, 10362–10367.
5 Hennrich, F. H.; Michel, R. H.; Fischer, A.; RichardSchneider, S.; Gilb, S.; Kappes, M. M.; Fuchs, D.; Burk, M.; Kobayashi, K.; Nagase, S. Isolation and characterization of $C_{80}$. *Angew. Chem., Int. Ed.* **1996**, *35*, 1732–1734.
6 Shinohara, H. Endohedral metallofullerenes. *Rep. Prog. Phys.* **2000**, *63*, 843–892.
7 Rodriguez-Fortea, A.; Balch, A. L.; Poblet, J. M. Endohedral metallofullerenes: A unique host-guest association. *Chem. Soc. Rev.* **2011**, *40*, 3551–3563.
8 Lu, X.; Akasaka, T.; Nagase, S. Chemistry of endohedral metallofullerenes: The role of metals. *Chem. Commun.* **2011**, *47*, 5942–5957.
9 Dunsch, L.; Yang, S. F. Endohedral clusterfullerenes: Playing with cluster and cage sizes. *Phys. Chem. Chem. Phys.* **2007**, *9*, 3067–3081.
10 Chaur, M. N.; Melin, F.; Ortiz, A. L.; Echegoyen, L. Chemical, electrochemical, and structural properties of endohedral metallofullerenes. *Angew. Chem., Int. Ed.* **2009**, *48*, 7514–7538.

11 Yamada, M.; Akasaka, T.; Nagase, S. Endohedral metal atoms in pristine and functionalized fullerene cages. *Acc. Chem. Res.* **2010**, *43*, 92–102.

12 Lu, X.; Akasaka, T.; Nagase, S. Carbide cluster metallofullerenes: Structure, properties, and possible origin. *Acc. Chem. Res.* **2013**, *46*, 1627–1635.

13 Zhang, J.; Stevenson, S.; Dorn, H. C. Trimetallic nitride template endohedral metallofullerenes: Discovery, structural characterization, reactivity, and applications. *Acc. Chem. Res.* **2013**, *46*, 1548–1557.

14 Popov, A. A.; Yang, S.; Dunsch, L. Endohedral fullerenes. *Chem. Rev.* **2013**, *113*, 5989–6113.

15 Garcia-Borràs, M.; Osuna, S.; Swart, M.; Luis, J. M.; Solà, M. Maximum aromaticity as a guiding principle for the most suitable hosting cages in endohedral metallofullerenes. *Angew. Chem., Int. Ed.* **2013**, *52*, 9275–9278.

16 Bethune, D. S.; Johnson, R. D.; Salem, J. R.; Devries, M. S.; Yannoni, C. S. Atoms in carbon cages: The structure and properties of endohedral fullerenes. *Nature* **1993**, *366*, 123–128.

17 Suzuki, T.; Maruyama, Y.; Kato, T.; Kikuchi, K.; Nakao, Y.; Achiba, Y.; Kobayashi, K.; Nagase, S. Electrochemistry and ab-initio study of the dimetallofullerene $La_2@C_{80}$. *Angew. Chem., Int. Ed.* **1995**, *34*, 1094–1096.

18 Akasaka, T.; Nagase, S.; Kobayashi, K.; Walchli, M.; Yamamoto, K.; Funasaka, H.; Kako, M.; Hoshino, T.; Erata, T. $^{13}C$ and $^{139}La$ NMR studies of $La_2@C_{80}$: First evidence for circular motion of metal atoms in endohedral dimetallofullerenes. *Angew. Chem., Int. Ed.* **1997**, *36*, 1643–1645.

19 Stevenson, S.; Rice, G.; Glass, T.; Harich, K.; Cromer, F.; Jordan, M. R.; Craft, J.; Hadju, E.; Bible, R.; Olmstead, M. M.; Maitra, K.; Fisher, A. J.; Balch, A. L.; Dorn, H. C. Small-band gap endohedral metallofullerenes in high yield and purity. *Nature* **1999**, *401*, 55–57.

20 Wang, C. R.; Kai, T.; Tomiyama, T.; Yoshida, T.; Kobayashi, Y.; Nishibori, E.; Takata, M.; Sakata, M.; Shinohara, H. A scandium carbide endohedral metallofullerene: $(Sc_2C_2)@C_{84}$. *Angew. Chem., Int. Ed.* **2001**, *40*, 397–399.

21 Liduka, Y.; Wakahara, T.; Nakahodo, T.; Tsuchiya, T.; Sakuraba, A.; Maeda, Y.; Akasaka, T.; Yoza, K.; Horn, E.; Kato, T.; Liu, M. T. H.; Mizorogi, N.; Kobayashi, K.; Nagase, S. Structural determination of metallofullerene $Sc_3C_{82}$ revisited: A surprising finding. *J. Am. Chem. Soc.* **2005**, *127*, 12500–12501.

22 Stevenson, S.; Mackey, M. A.; Stuart, M. A.; Phillips, J. P.; Easterling, M. L.; Chancellor, C. J.; Olmstead, M. M.; Balch, A. L. A distorted tetrahedral metal oxide cluster inside an icosahedral carbon cage. Synthesis, isolation, and structural characterization of $Sc_4(\mu_3\text{-}O)_2@I_h\text{-}C_{80}$. *J. Am. Chem. Soc.* **2008**, *130*, 11844–11845.

23 Wang, T. S.; Feng, L.; Wu, J. Y.; Xu, W.; Xiang, J. F.; Tan, K.; Ma, Y. H.; Zheng, J. P.; Jiang, L.; Lu, X.; Shu, C. Y.; Wang, C. R. Planar quinary cluster inside a fullerene cage: Synthesis and structural characterizations of $Sc_3NC@C_{80}\text{-}I_h$. *J. Am. Chem. Soc.* **2010**, *132*, 16362–16364.

24 Fu, W. J.; Zhang, J. Y.; Fuhrer, T.; Champion, H.; Furukawa, K.; Kato, T.; Mahaney, J. E.; Burke, B. G.; Williams, K. A.; Walker, K.; Dixon, C.; Ge, J. C.; Shu, C. Y.; Harich, K.; Dorn, H. C. $Gd_2@C_{79}N$: Isolation, characterization, and monoadduct formation of a very stable heterofullerene with a magnetic spin state of S = 15/2. *J. Am. Chem. Soc.* **2011**, *133*, 9741–9750.

25 Zuo, T. M.; Xu, L. S.; Beavers, C. M.; Olmstead, M. M.; Fu, W. J.; Crawford, D.; Balch, A. L.; Dorn, H. C. $M_2@C_{79}N$ (M = Y, Tb): Isolation and characterization of stable endohedral metallofullerenes exhibiting M−M bonding interactions inside aza[80]fullerene cages. *J. Am. Chem. Soc.* **2008**, *130*, 12992–12997.

26 Mercado, B. Q.; Olmstead, M. M.; Beavers, C. M.; Easterling, M. L.; Stevenson, S.; Mackey, M. A.; Coumbe, C. E.; Phillips, J. D.; Phillips, J. P.; Poblet, J. M.; Balch, A. L. A seven atom cluster in a carbon cage, the crystallographically determined structure of $Sc_4(\mu_3\text{-}O)_3@I_h\text{-}C_{80}$. *Chem. Commun.* **2010**, *46*, 279–281.

27 Popov, A. A.; Zhang, L.; Dunsch, L. A pseudoatom in a cage: Trimetallofullerene $Y_3@C_{80}$ mimics $Y_3N@C_{80}$ with nitrogen substituted by a pseudoatom. *ACS Nano* **2010**, *4*, 795–802.

28 Xu, W.; Feng, L.; Calvaresi, M.; Liu, J.; Liu, Y.; Niu, B.; Shi, Z. J.; Lian, Y. F.; Zerbetto, F. An experimentally observed trimetallofullerene $Sm_3@I_h\text{-}C_{80}$: Encapsulation of three metal atoms in a cage without a nonmetallic mediator. *J. Am. Chem. Soc.* **2013**, *135*, 4187–4190.

29 Chen, C. B.; Liu, F. P.; Li, S. J.; Wang, N.; Popov, A. A.; Jiao, M. Z.; Wei, T.; Li, Q. X.; Dunsch, L.; Yang, S. F. Titanium/yttrium mixed metal nitride clusterfullerene $TiY_2N@C_{80}$: Synthesis, isolation, and effect of the group-III metal. *Inorg. Chem.* **2012**, *51*, 3039–3045.

30 Osuna, S.; Rodriguez-Fortea, A.; Poblet, J. M.; Sola, M.; Swart, M. Product formation in the Prato reaction on $Sc_3N@D_{5h}\text{-}C_{80}$: Preference for [5,6]-bonds, and not pyracylenic bonds. *Chem. Commun.* **2012**, *48*, 2486–2488.

31 Osuna, S.; Valencia, R.; Rodriguez-Fortea, A.; Swart, M.; Sola, M.; Poblet, J. M. Full exploration of the Diels-Alder cycloaddition on metallofullerenes $M_3N@C_{80}$ (M=Sc, Lu, Gd): The $D_{5h}$ versus $I_h$ isomer and the influence of the metal cluster. *Chem. −Eur. J.* **2012**, *18*, 8944–8956.

32 Garcia-Borràs, M.; Osuna, S.; Luis, J. M.; Swart, M.; Solà, M. A Complete Guide on the Influence of Metal Clusters in the Diels-Alder Regioselectivity of $I_h\text{-}C_{80}$ Endohedral Metallofullerenes. *Chem.—Eur. J.* **2013**, *19*, 14931–14940.

33 Osuna, S.; Swart, M.; Sola, M. The reactivity of endohedral fullerenes. What can be learnt from computational studies? *Phys. Chem. Chem. Phys.* **2011**, *13*, 3585–3603.

34 Chen, N.; Zhang, E. Y.; Wang, C. R. $C_{80}$ encaging four different atoms: The synthesis, isolation, and characterizations of $ScYErN@C_{80}$. *J. Phys. Chem. B* **2006**, *110*, 13322–13325.

35 Tan, K.; Lu, X. Electronic structure and redox properties of the open-shell metal-carbide endofullerene $Sc_3C_2@C_{80}$: A density functional theory investigation. *J. Phys. Chem. A* **2006**, *110*, 1171–1176.

36 Nishibori, E.; Terauchi, I.; Sakata, M.; Takata, M.; Ito, Y.; Sugai, T.; Shinohara, H. High-resolution analysis of $(Sc_3C_2)@C_{80}$ metallofullerene by third generation synchrotron radiation X-ray powder diffraction. *J. Phys. Chem. B* **2006**, *110*, 19215–19219.

37 Krause, M.; Ziegs, F.; Popov, A. A.; Dunsch, L. Entrapped bonded hydrogen in a fullerene: The five-atom cluster $Sc_3CH$ in $C_{80}$. *ChemPhysChem* **2007**, *8*, 537–540.

38 Wang, T. S.; Chen, N.; Xiang, J. F.; Li, B.; Wu, J. Y.; Xu, W.; Jiang, L.; Tan, K.; Shu, C. Y.; Lu, X.; Wang, C. R. Russian-doll-type metal carbide endofullerene: Synthesis, isolation, and characterization of $Sc_4C_2@C_{80}$. *J. Am. Chem. Soc.* **2009**, *131*, 16646–16647.

39 Tan, K.; Lu, X.; Wang, C. R. Unprecedented $\mu_4\text{-}C_2^{\,6-}$ anion in $Sc_4C_2@C_{80}$. *J. Phys. Chem. B* **2006**, *110*, 11098–11102.

40 Valencia, R.; Rodriguez-Fortea, A.; Stevenson, S.; Balch, A. L.; Poblet, J. M. Electronic structures of scandium oxide endohedral metallofullerenes, $Sc_4(\mu_3\text{-}O)_n@I_h\text{-}C_{80}$ (n = 2, 3). *Inorg. Chem.* **2009**, *48*, 5957–5961.

41 Jin, P.; Zhou, Z.; Hao, C.; Gao, Z. X.; Tan, K.; Lu, X.; Chen, Z. F. NC unit trapped by fullerenes: A density functional theory study on $Sc_3NC@C_{2n}$ (2n = 68, 78, and 80). *Phys. Chem. Chem. Phys.* **2010**, *12*, 12442–12449.

42 Feng, Y. Q.; Wang, T. S.; Wu, J. Y.; Ma, Y. H.; Zhang, Z. X.; Jiang, L.; Ge, C. H.; Shu, C. Y.; Wang, C. R. Spin-active metallofullerene stabilized by the core of an NC moiety. *Chem. Commun.* **2013**, *49*, 2148–2150.

43 Wu, J. Y.; Wang, T. S.; Ma, Y. H.; Jiang, L.; Shu, C. Y.; Wang, C. R. Synthesis, isolation, characterization, and theoretical studies of $Sc_3NC@C_{78}\text{-}C_2$. *J. Phys. Chem. C* **2011**, *115*, 23755–23759.

44 Yang, S. F.; Chen, C. B.; Liu, F. P.; Xie, Y. P.; Li, F. Y.; Jiao, M. Z.; Suzuki, M.; Wei, T.; Wang, S.; Chen, Z. F.; Lu, X.; Akasaka, T. An improbable monometallic cluster entrapped in a popular fullerene cage: $YCN@C_s(6)\text{-}C_{82}$. *Sci. Rep.* **2013**, *3*, 1487.

45 Hummelen, J. C.; Knight, B.; Pavlovich, J.; Gonzalez, R.; Wudl, F. Isolation of the heterofullerene $C_{59}N$ as its dimer $(C_{59}N)_2$. *Science* **1995**, *269*, 1554–1556.

46 Stevenson, S.; Ling, Y.; Coumbe, C. E.; Mackey, M. A.; Confait, B. S.; Phillips, J. P.; Dorn, H. C.; Zhang, Y. Preferential encapsulation and stability of $La_3N$ cluster in 80 atom cages: Experimental synthesis and computational investigation of $La_3N@C_{79}N$. *J. Am. Chem. Soc.* **2009**, *131*, 17780–17782.

47 Rodriguez-Fortea, A.; Campanera, J. M.; Cardona, C. M.; Echegoyen, L.; Poblet, J. M. Dancing on a fullerene surface: Isomerization of $Y_3N@$(N-ethylpyrrolidino-$C_{80}$) from the 6,6 to the 5,6 regioisomer. *Angew. Chem., Int. Ed.* **2006**, *45*, 8176–8180.

48 Chen, N.; Fan, L. Z.; Tan, K.; Wu, Y. Q.; Shu, C. Y.; Lu, X.; Wang, C. R. Comparative spectroscopic and reactivity studies of $Sc_{3-x}Y_xN@C_{80}$ (x = 0−3). *J. Phys. Chem. C* **2007**, *111*, 11823–11828.

49 Chen, N.; Zhang, E. Y.; Tan, K.; Wang, C. R.; Lu, X. Size effect of encaged clusters on the exohedral chemistry of endohedral fullerenes: A case study on the pyrrolidino reaction of $Sc_xGd_{3-x}N@C_{80}$ (x = 0−3). *Org. Lett.* **2007**, *9*, 2011–2013.

50 Yang, S. F.; Popov, A. A.; Chen, C. H.; Dunsch, L. Mixed metal nitride clusterfullerenes in cage isomers: $Lu_xSc_{3-x}N@C_{80}$ (x = 1, 2) as compared with $M_xSc_{3-x}N@C_{80}$ (M = Er, Dy, Gd, Nd). *J. Phys. Chem. C* **2009**, *113*, 7616–7623.

51 Yang, S. F.; Popov, A. A.; Dunsch, L. Carbon pyramidalization in fullerene cages induced by the endohedral cluster: Non-scandium mixed metal nitride clusterfullerenes. *Angew. Chem., Int. Ed.* **2008**, *47*, 8196–8200.

52 Morton, J. J. L.; Tiwari, A.; Dantelle, G.; Porfyrakis, K.; Ardavan, A.; Briggs, G. A. D. Switchable $ErSc_2N$ rotor within a $C_{80}$ fullerene cage: An electron paramagnetic resonance and photoluminescence excitation study. *Phys. Rev. Lett.* **2008**, *101* (1), No. 013002.

53 Nafradi, B.; Antal, A.; Pasztor, A.; Forro, L.; Kiss, L. F.; Feher, T.; Kovats, E.; Pekker, S.; Janossy, A. Molecular and spin dynamics in the paramagnetic endohedral fullerene $Gd_3N@C_{80}$. *J. Phys. Chem. Lett.* **2012**, *3*, 3291–3296.

54 Yang, S. F.; Chen, C. B.; Popov, A. A.; Zhang, W. F.; Liu, F. P.; Dunsch, L. An endohedral titanium(III) in a clusterfullerene: putting a non-group-III metal nitride into the $C_{80}\text{-}I_h$ fullerene cage. *Chem. Commun.* **2009**, *42*, 6391–6393.

55 Kurihara, H.; Iiduka, Y.; Rubin, Y.; Waelchli, M.; Mizorogi, N.; Slanina, Z.; Tsuchiya, T.; Nagase, S.; Akasaka, T. Unexpected formation of a $Sc_3C_2@C_{80}$ bisfulleroid derivative. *J. Am. Chem. Soc.* **2012**, *134*, 4092–4095.

56 Wang, T. S.; Wu, J. Y.; Xu, W.; Xiang, J. F.; Lu, X.; Li, B.; Jiang, L.; Shu, C. Y.; Wang, C. R. Spin divergence induced by exohedral modification: ESR study of $Sc_3C_2@C_{80}$ fulleropyrrolidine. *Angew. Chem., Int. Ed.* **2010**, *49*, 1786–1789.

57 Wang, T. S.; Wu, J. Y.; Feng, Y. Q.; Ma, Y. H.; Jiang, L.; Shu, C. Y.; Wang, C. R. Preparation and ESR study of $Sc_3C_2@C_{80}$ bis-addition fulleropyrrolidines. *Dalton Trans.* **2012**, *41*, 2567–2570.

58 Ma, Y. H.; Wang, T. S.; Wu, J. Y.; Feng, Y. Q.; Jiang, L.; Shu, C. Y.; Wang, C. R. Susceptible electron spin adhering to an yttrium cluster inside an azafullerene $C_{79}N$. *Chem. Commun.* **2012**, *48*, 11570–11572.

59 Jakes, P.; Dinse, K. P. Chemically induced spin transfer to an encased molecular cluster: An EPR study of $Sc_3N@C_{80}$ radical anions. *J. Am. Chem. Soc.* **2001**, *123*, 8854–8855.

60 Popov, A. A.; Chen, N.; Pinzon, J. R.; Stevenson, S.; Echegoyen, L. A.; Dunsch, L. Redox-active scandium oxide cluster inside a fullerene cage: Spectroscopic, voltammetric, electron spin resonance spectroelectrochemical, and extended density functional theory study of $Sc_4O_2@C_{80}$ and its ion radicals. *J. Am. Chem. Soc.* **2012**, *134*, 19607–19618.